

- [3] J. C. Miller, R. L. Mowery, E. R. Krausz, S. M. Jacobs, H. W. Kim, P. N. Schatz, and L. Andrews, *J. Chem. Phys.* **74**, 6349 (1981).
- [4] J. H. Ammeter and D. C. Schlosnagle, *J. Chem. Phys.* **59**, 4784 (1973).
- [5] M. Moskovits and J. E. Hulse, *J. Chem. Phys.* **66**, 3988 (1977).
- [6] R. Grinter and D. R. Stern, in print.
- [7] L. Brewer and C. A. Chang, *J. Chem. Phys.* **56**, 1728 (1972).
- [8] L. Brewer and A. W. Searcy, *J. Am. Chem. Soc.* **73**, 5308 (1951).
- [9] R. F. Porter, P. Schissel, and M. G. Inghram, *J. Chem. Phys.* **23**, 339 (1955).
- [10] R. Grinter and D. R. Stern, paper presented at the 3rd Int. Conf. on Matrix Isolation Spectroscopy, Nottingham 1981.
- [11] We are grateful to Dr. J. P. Urban for performing the mass spectroscopy measurements.
- [12] See, e.g., D. Nagel and B. Sonntag, *Ber. Bunsenges. Phys. Chem.* **82**, 38 (1978).
- [13] F. Forstmann, D. M. Kolb, D. Leutloff, and W. Schulze, *J. Chem. Phys.* **66**, 2806 (1977).
- [14] J. Hormes, R. Grinter, B. Breithaupt, and D. M. Kolb, *J. Chem. Phys.* **78**, 158 (1983).
- [15] N. P. Penkin and L. N. Shabanova, *Opt. Spectrosc.* **18**, 504 (1964).
- [16] F. Forstmann and S. Ossicini, *J. Chem. Phys.* **73**, 5997 (1980).
- [17] D. S. Ginter, M. L. Ginter, and K. K. Innes, *Astrophys. J.* **139**, 365 (1964).
- [18] J. C. Miller, B. S. Ault, and L. Andrews, *J. Chem. Phys.* **67**, 2478 (1977).

(Eingegangen am 16. Februar 1983)

E 5384

Arrhenius Parameters for the Reactions of O Atoms with Some Alkynes in the Range 300–1300 K

K. H. Homann and Ch. Wellmann

Institut für Physikalische Chemie der Technischen Hochschule Darmstadt, Petersenstraße 20, D-6100 Darmstadt

Freie Radikale / Kohlenwasserstoffe / Reaktionskinetik

The rates of the reactions of oxygen atoms with acetylene (1), propyne (2), 1–3-butadiyne (3), 1-buten-3-yne (4), and 1-butyne (5) in a discharge flow system have been measured in the temperature range $300 < T < 1300$ K. – The Arrhenius expressions for the respective bimolecular rate constants are

$$k_1/\text{cm}^3 \text{ mol}^{-1} \text{ s}^{-1} = (1.6 \pm 0.5) \cdot 10^{13} \exp\left(-\frac{1550 \text{ K}}{T}\right)$$

$$k_2/\text{cm}^3 \text{ mol}^{-1} \text{ s}^{-1} = (1.5 \pm 0.4) \cdot 10^{13} \exp\left(-\frac{1060 \text{ K}}{T}\right)$$

$$k_3/\text{cm}^3 \text{ mol}^{-1} \text{ s}^{-1} = (2.8 \pm 0.6) \cdot 10^{13} \exp\left(-\frac{870 \text{ K}}{T}\right)$$

$$k_4/\text{cm}^3 \text{ mol}^{-1} \text{ s}^{-1} = (3.0 \pm 1.1) \cdot 10^{13} \exp\left(-\frac{910 \text{ K}}{T}\right)$$

$$k_5/\text{cm}^3 \text{ mol}^{-1} \text{ s}^{-1} = (2.3 \pm 0.7) \cdot 10^{13} \exp\left(-\frac{870 \text{ K}}{T}\right).$$

There is a correlation between the activation energies and the ionization potentials of the alkynes.

1. Introduction

In the reaction of O atoms with an excess of acetylene [1, 2] as well as in the fuel-rich flames of hydrocarbons a variety of higher alkynes is formed both as intermediates and more or less as final products [2]. They also play a role as the first low molecular mass unsaturated hydrocarbons in the reactions that finally lead to polycyclic aromatic hydrocarbons and soot in fuel-rich combustion. The main reaction partners of these alkynes in combustion systems are H, O, and OH-radicals. Of these species the oxygen atoms give products that can most easily lead to still higher alkynes and other unsaturated high molecular mass products. For the mechanistic understanding and a quantitative simulation of these complicated reaction systems it is necessary to know the rates of consecutive reactions of the alkynic intermediates. Therefore, we have measured reaction rates of oxygen atoms with acetylene C_2H_2 ,

propyne C_3H_4 , 1–3-butadiyne C_4H_2 , 1-buten-3-yne C_4H_4 , 1-butyne C_4H_6 in a temperature range between 300 and 1300 K. All of these reactions have been studied before but with the exception of C_2H_2 the temperature regimes had been much smaller.

2. Experimental

2.1. The Reactor

The measurements were done using a high temperature, low pressure discharge flow system, in principle similar to the one described in Ref. [3]. The analysis of reactants and products was performed by means of a nozzle-beam sampling system coupled to a quadrupole mass spectrometer. The arrangement of both units is shown in Fig. 1. The reactants were diluted with helium which simultaneously served as a heat bath into which the O atoms and the hydrocarbon were injected. For preheating, the helium streamed through a furnace equipped with three MoSi_2 -heating elements and an auxiliary heating coil on the outside of the 138 mm wide and 370 mm long aluminium oxide tube. This

preheating furnace was connected to the reactor tube by a nozzle-like piece of refractory material. The flow reactor consisted of a quartz tube of 26 mm inner diameter and 185 mm length. It was surrounded by a heat resisting steel tube to obtain a good axial temperature profile and also equipped with two auxiliary heating coils on the outside. The temperature was controlled and regulated through Pt-PtRh-thermocouples in the preheating furnace and between the quartz and the steel tube of the reactor. The preheating furnace and the reactor were thermally insulated by Fiberfrax ceramic isolation wool and mounted inside a vacuum tight stainless steel cylinder which was flanged onto the molecular beam system.

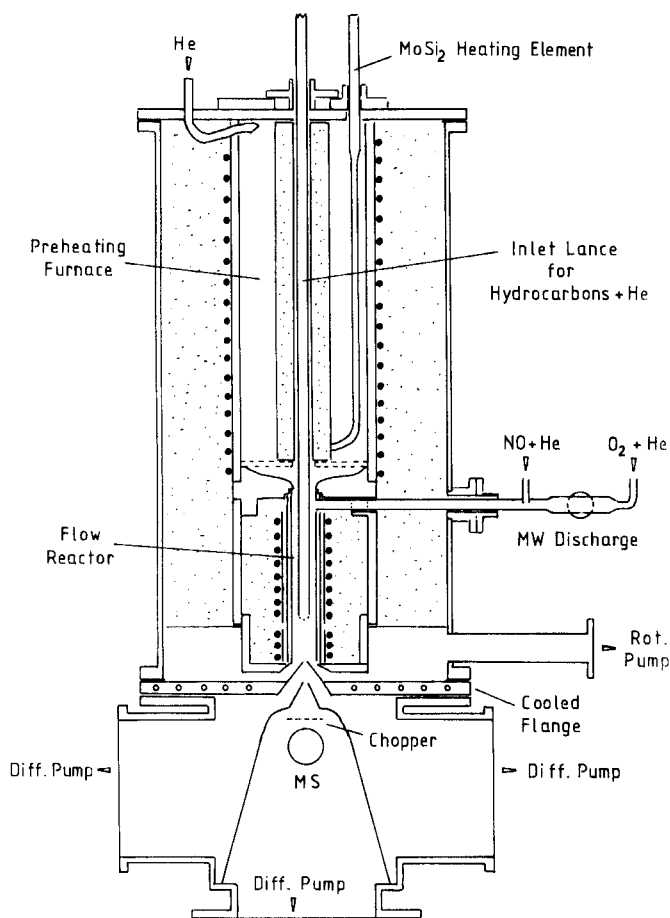


Fig. 1

High temperature discharge flow reactor and molecular beam sampling system with quadrupole mass spectrometer. (Scale 1 : 5, half schematic)

Oxygen atoms were generated by a 2.45 GHz microwave discharge in oxygen-helium mixtures ($1:20$ to $1:2 \cdot 10^3$) and also by the titration reaction $N + NO \rightarrow N_2 + O$ in a side tube to the reactor.

The hydrocarbon was admitted to the reactor by means of an axially movable inlet lance. To prevent a disturbance of the temperature profile in the reactor this lance had to be heated at its lower end to the same temperature as the reactor walls. The end protruding into the reactor was covered with a thin quartz tube of 12 mm diameter to minimize wall effects on the reaction rates. Its inside, however, was water-cooled to avoid pyrolysis of the alkynes before entering the reactor. The inlet lance went through the preheating furnace being led by a thermally insulated aluminium oxide tube which also served as a radiation shield.

The chopped-molecular-beam sampling system with the mass spectrometer has been described previously [4]. Its set-up can be seen from Fig. 1. An electron energy of nominal 25 eV turned out to be a good compromise between the sensitivity of the ion source and the production of fragment ions. A product concentration down to about $5 \cdot 10^{-14}$ mol cm $^{-3}$ corresponding to a mole fraction of less than 10^{-6} in the reactor could be detected.

2.2. Operation and Measuring Conditions

The gas flows were regulated through needle valves. While capillary flow meters were used for the helium, all other gases, the volume flow rates of which lay between 10^{-2} and 1 cm 3 s $^{-1}$, were admitted through special manostats described earlier [5]. Before any measurements at high temperatures were done the preheating furnace and the reactor had to be heated up slowly during 4–8 hours to prevent breaking of the ceramic parts. After another two hours during which the flow rate of helium, the temperature profile in the reactor, and the flows of the reactants were adjusted to the desired values the measurements were performed by moving the inlet lance to different positions along the reactor axis and measuring the reactant and product concentrations at the end of the reactor.

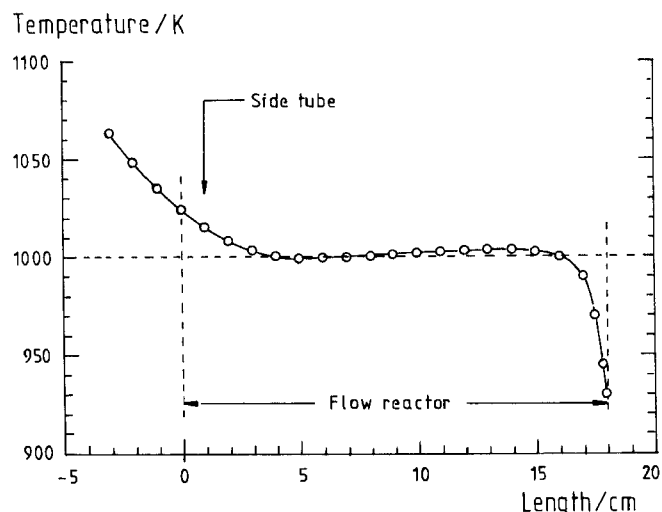


Fig. 2

Temperature profile in the flow reactor for a nominal temperature of 1000 K

Fig. 2 shows the temperature profile in the flow reactor for a set temperature of 1000 K. The helium leaving the preheating furnace had to be heated to a temperature about 10% higher than that of the reactor to avoid a temperature minimum at the position of the side tube. The cool helium flowing through the side tube together with the oxygen atoms amounted to 10–15% of the total through-put. Along the last 2–3 cm of the reactor the temperature decreased to about 10% below the nominal value. This was caused by heat conduction to the cooled flange and could only be incompletely compensated by an auxiliary heating coil around the end of the reactor.

The total pressure in the reactor was constantly set to 2.7 mbar (2.0 Torr). The O atom concentration at the entrance end of the flow reactor was always of the order of $5 \cdot 10^{-11}$ mol cm $^{-3}$.

Table 1
Materials and Purities

Substance	Source	Purity
Acetylene (C $_2$ H $_2$)	Linde	99.6 (no acetone)
Propyne (C $_3$ H $_4$)	Baker	99.4
1–3 Butadiyne (C $_4$ H $_2$)	own synthesis	99
1-Buten-3-yne (C $_4$ H $_4$)	Chem. Werke Hüls	99
1-Butyne (C $_4$ H $_6$)	Baker	97.4
Oxygen	Messer-Griesheim	99.995
Nitrogenoxide (NO)	Matheson	98.5
Helium	Messer-Griesheim	99.996

2.3. Substances and Calibration

A survey of the substances used and their purities is given in Table 1. Trace water vapor of the helium was frozen out by two liquid N $_2$ cooled traps. 1–3-butadiyne was prepared according to Ref. [6] and purified

twice through sublimation. For mass spectrometric calibration a known flow rate of the substances was let through the inlet lance and their mass spectrometric sensitivities measured under the same conditions as for the kinetic experiments but without O atoms. Calibrations were repeated before each series of measurements.

2.4. Wall Recombination of Oxygen Atoms

The concentration of oxygen atoms was obtained from the decrease of the O₂ signal when the discharge was on. However, the recombination of O atoms at the reactor walls had to be taken into account, especially at the higher temperatures. The quartz tube of the reactor was rinsed with 5% HF solution to reduce the wall recombination coefficient which was determined before each series of measurements. This was achieved by varying the flow rate of the mixture of helium and oxygen atoms (without alkyne) through the reactor while keeping the conditions of O₂ concentration, flow rate, and pressure in the discharge constant. A variation of the total throughput caused a change in concentration of the O atoms and the variation of the flow velocity brought about a corresponding change in the residence time in the reactor. The first order rate constant k_w was obtained from the expression

$$k_w = - \frac{\ln \frac{I_A \dot{V}_A}{I_B \dot{V}_B}}{t_A - t_B}$$

where I , \dot{V} and t are the mass spectrometric signal for O atoms, the volume flow rate, and the residence time, respectively, and the subscripts A and B refer to two different settings.

The measurements were done over a range of $295 < T < 1000$ K. The temperature dependence of k_w roughly obeys an Arrhenius law. However, due to the varying wall conditions through frequent heating, cooling, and exchange of the quartz tube a comparatively broad range of parameters resulted on the long time average:

$$k_w/\text{s}^{-1} = 1.0 \cdot 10^3 \exp\left(-\frac{1300 \text{ K}}{T}\right)$$

corresponding to an apparent energy of activation of 11 ± 3.3 kJ mol⁻¹. This dependence must be considered as intrinsic for this special high temperature flow reactor and the working conditions. It can hardly be compared to results with other quartz reactors [7–9]. The reason for this may be a very thin film of hydrocarbon polymer which forms on the wall as soon as an excess of alkyne reacts with the O atoms.

3. Results

For the reaction of oxygen atoms with different hydrocarbons HC_{*i*} the general rate law

$$-\frac{d[\text{O}]}{dt} = n_i \cdot k_i(T) [\text{HC}_i] [\text{O}]$$

has been applied. n_i is the number of O atoms consumed per number of hydrocarbon molecules i reacted;

$$n_i = \frac{\Delta[\text{O}]}{\Delta[\text{HC}_i]}$$

n_i is determined using an excess of hydrocarbon concentration in the reaction mixture. It is little dependent on temperature but more or less on the mixture ratio. For the kinetic experiments an excess of hydrocarbon was always applied, sufficient to allow an evaluation of the rate constant under pseudo-first-order conditions.

3.1. O + Acetylene → Products (1)

In the reaction $\text{O} + \text{C}_2\text{H}_2$ n_1 has been reported to be 2 [10, 11, 13, 14]. This was confirmed and it was found that it is practically constant in the range 295–1330 K. It decreases to 1.8 at very large initial concentration ratios $[\text{C}_2\text{H}_2]_0/[\text{O}]_0 > 50$ [11].

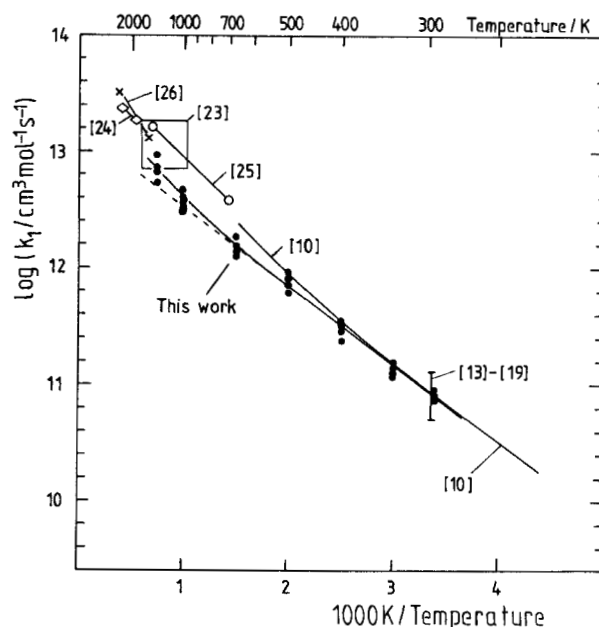


Fig. 3
Arrhenius diagram for the rate constant k_1 of the reaction
 $\text{O} + \text{C}_2\text{H}_2 \rightarrow \text{products}$

Fig. 3 shows the results for k_1 from this work in form of an Arrhenius diagram in which the results of some other investigators have also been plotted. There is good agreement with other values in the range between 300 and 500 K. Between 500 and 1300 K our results come out somewhat lower but they confirm previous reports that there is a curvature in the Arrhenius plot becoming noticeable above about 500 K. In the range from room temperature and lower to ≈ 500 K k_1 can well be described by the equation

$$k_1/\text{cm}^3 \text{ mol}^{-1} \text{ s}^{-1} = (1.6 \pm 0.5) \cdot 10^{13} \exp\left(-\frac{1550 \text{ K}}{T}\right)$$

corresponding to an apparent activation energy of 12.9 ± 0.6 kJ mol⁻¹. This expression, however, cannot be used for extrapolation to higher temperatures or even flame temperatures. There the apparent activation energy seems to be more than double the low temperature value. One of the reasons for this is most probably the opening of further reaction channels such as



which also seems to contribute by about 3% to the room temperature channel ($\rightarrow \text{CH}_2 + \text{CO}$) [14].

At the highest temperatures



which does not occur at low temperatures might also contribute to the conversion of acetylene.

3.2. O + Propyne → Products (2)

The rate constant for this reaction has been measured in the temperature range 295 to 1330 K using an excess of C₃H₄ between 5- and 30-fold. The number n_2 of O atoms consumed per C₃H₄ molecule was found to be 1.9 ± 0.2 which agrees fairly well with that of El-Dessouky (1.8 ± 0.1 [27]) and Herbrechtsmeier and Wagner (2.2 [28]). Thus, it is nearly the same as for acetylene and it has been set equal to 2 for the evaluation of the rate constant. The temperature dependence is again demonstrated in an Arrhenius diagram together with results from the literature. In this case a curvature is not noticeable and a least square fit gives the expression

$$k_2/\text{cm}^3 \text{ mol}^{-1} \text{ s}^{-1} = (1.5 \pm 0.4) \cdot 10^{13} \exp\left(-\frac{1060 \text{ K}}{T}\right)$$

corresponding to an experimental energy of activation of (8.8 ± 1.2) kJ mol⁻¹ (see Fig. 4).

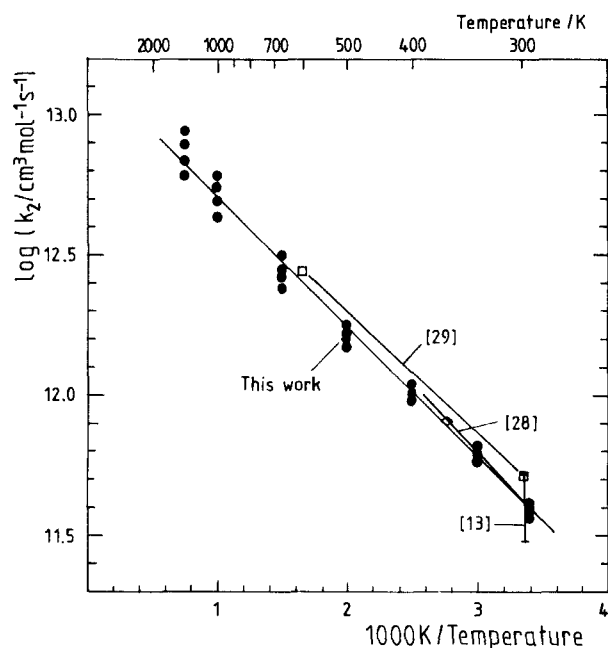


Fig. 4

Arrhenius diagram for the rate constant k_2 of the reaction
O + propyne → products

Products of the reaction are CO, C₂H₄ and C₂H₂ in agreement with Ref. [28] together with less amounts of C₂H₆ and C₃H₆.

3.3. O + 1-3-Butadiyne → Products (3)

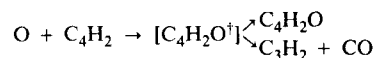
This reaction has been studied previously only by two working groups in a very limited temperature regime [30, 31]. In this work the range was extended to 1000 K. The excess of C₄H₂ over O atoms was chosen between 5- and 20-fold in which range n_3 is ≈ 1.7 decreasing slightly towards richer mixtures [31]. No curvature of the Arrhenius plot could be found and a least square evaluation leads to the expression

$$k_3/\text{cm}^3 \text{ mol}^{-1} \text{ s}^{-1} = (2.8 \pm 0.6) \cdot 10^{13} \exp\left(-\frac{870 \text{ K}}{T}\right)$$

from which an apparent activation energy of (7.2 ± 0.7) kJ mol⁻¹ is derived. In addition to the products CO, C₂H₂, C₆H₂, C₃H₄, C₄H₄, C₇H₄ and a product of a mass of 42 u, the hydrocarbons C₃H₄ and C₆H₄, C₈H₂ and C₁₀H₂ have been observed in low concentrations.

An additional investigation of the primary products of the reaction O + C₄H₂ was done by means of a crossed jet reactor and molecular beam mass spectrometric analysis in cooperation with K. Hoyer, University of Göttingen. The apparatus and the method used are described in Ref. [12].

Fig. 6 shows the mass spectrometric intensities of the products observed using 19.5 eV electron energy for the ionization. From these results it can be deduced that the reaction channel



is the dominant one. Because of the lack of mass spectrometric sensitivities for the different species no percentages for the contribution of different channels can be given. In view of the low pressure in the jet reactor (ca. 0.3 mbar) it must be assumed that a greater part of the excited intermediate C₄H₂O[†] is deactivated at the wall before reaching the ion source. The presence of C₂H₂ is due to the very fast consecutive reaction

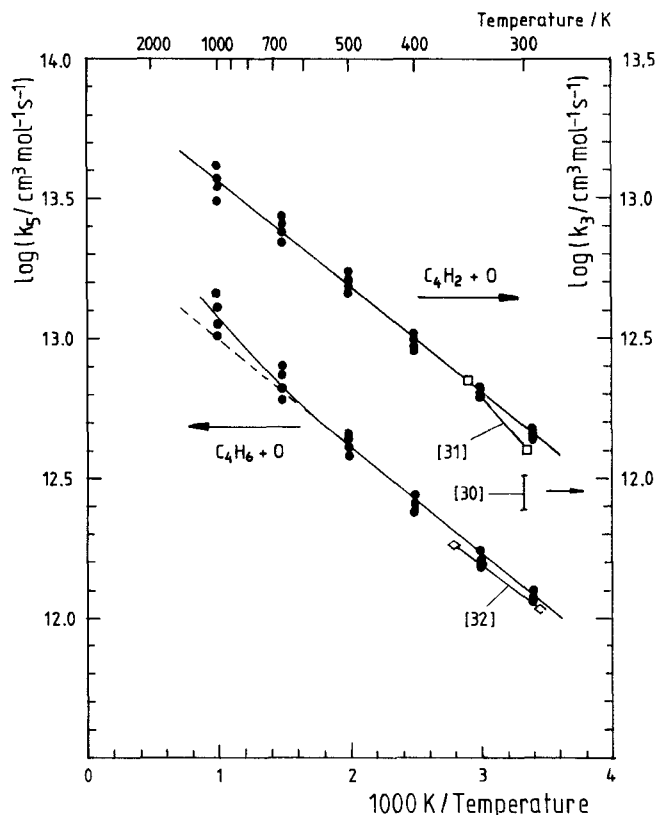


Fig. 5

Arrhenius diagram for the rate constants k_3 of the reaction
O + C₄H₂ → products and k_5 of the reaction O + 1-Butyne → products

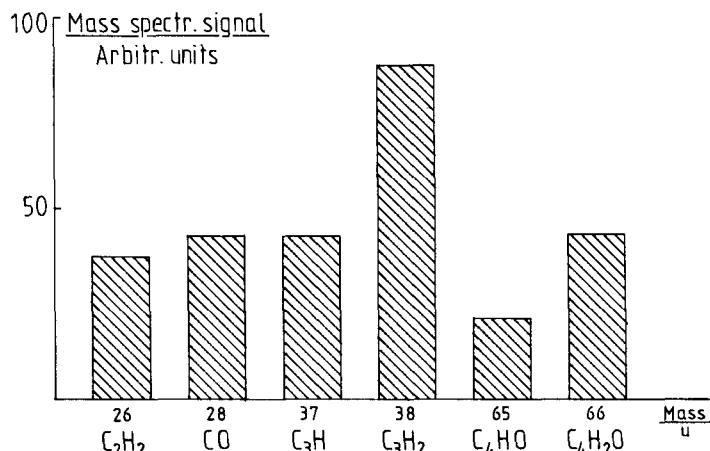


Fig. 6

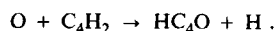
Mass spectrum of the primary products of the reaction O + C₄H₂

for which a rate constant of about $8 \cdot 10^{13}$ cm³ mol⁻¹ s⁻¹ or higher has been postulated [1]. There is no contribution of the reaction channel



since C₂O is not amongst the primary products.

C₃H⁺ most probably is a fragment ion of C₃H₂⁺ since no HCO⁺ could be detected. The presence of HC₄O⁺ which partly comes from fragmentation of C₄H₂O⁺ suggests a smaller contribution of the reaction route



It is estimated that this contribution is less than 10 percent. These measurements confirm the previously used mechanism for the reaction system O + C₄H₂ [30, 31].

3.4. O + 1-Buten-3-yne → Products (4)

For this reaction only one room temperature value for k_4 exists which has been obtained from measurements with an excess of O atoms [31]. In the present work a 5- to 10-fold excess of C_4H_4 has been applied. The stoichiometric number n_4 is 1.9 for the fivefold and 1.5 for the tenfold excess. Measurements could only be made at 295 and 500 K because of the small amount of C_4H_4 that was at our disposal. If Arrhenius behaviour is adopted in this range the corresponding equation is

$$k_4/\text{cm}^3 \text{ mol}^{-1} \text{ s}^{-1} = (3.0 \pm 1.1) \cdot 10^{13} \exp\left(-\frac{910 \text{ K}}{T}\right)$$

with an energy of activation of $7.6 \pm 0.8 \text{ kJ mol}^{-1}$.

3.5. O + 1-Butyne → Products (5)

This reaction has been studied by Herbrechtsmeier and Wagner [32] who used both an excess of hydrocarbon and oxygen atoms, respectively, in the range $290 < T < 357 \text{ K}$. We have extended this range to 1000 K working with an excess of 1-butyne. n_5 is 2.4 at an 8-fold excess of 1-butyne and decreases to 2.0 at a 24-fold excess. Fig. 5 shows an Arrhenius diagram giving also the reported plot of Ref. [32] which deviates only slightly from these results. There seems to be a slight variation from an Arrhenius behaviour noticeable above 500 K. For the almost linear part between 290 and 500 K an expression

$$k_5/\text{cm}^3 \text{ mol}^{-1} \text{ s}^{-1} = (2.3 \pm 0.7) \cdot 10^{13} \exp\left(-\frac{870 \text{ K}}{T}\right);$$

$E_a = 7.2 \pm 0.7 \text{ kJ mol}^{-1}$ describes the results.

4. Concluding Remarks

It is remarkable that the rate constants of the reaction of O atoms with all the C_4 -alkynes are the same within the limits of experimental error over a considerable range of temperatures. This can be explained by the fact that the primary reaction channel is the same for all these C_4 -alkynes as it is also for propyne and acetylene itself. This was shown by Hoyermann and co-workers [12] and in the case of C_4H_2 in this work. It consists of a decomposition of the excited addition complex (O-alkyne) into CO and a carbene. The identical activation energies of the reaction of the C_4 -alkynes can be compared with the very similar ionization potentials of the hydrocarbons since oxygen atoms are electrophilic reactants. Herron et al. correlated the energies of activation of the reaction of oxygen atoms with alkenes to the respective ionization potentials including acetylene in this series [33]. These measurements show that there is also a correlation in this sense for the alkynes but they do not fall onto the same line as the alkenes (see Fig. 7). 1-Buten-3-yne behaves much more like an alkyne with respect to both the primary reaction channel and the rate constant. Negative energies of activation as with the larger alkenes [34] are not observed for the alkynes.

The reaction system O + alkyne in hydrocarbon-rich mixtures is complicated through many consecutive reactions of the carbene with O and H atoms and with the alkyne reactant. This leads to a variety of other unsaturated hydrocarbons as was shown in the case of C_2H_2 [1] and the other alkynes [28, 31, 32] for the reaction near room temperature. A detailed investigation of the development of the product concentration profiles at higher temperatures has not been undertaken for the higher alkynes in this work. However, inspection of the product mass spectra of the C_3H_4 and the C_4 -alkyne reactions with O atoms at high temperatures did not show a dramatic change in the

product spectra as compared to those near room temperature. These have been reported by several authors. The main purpose of the present measurements was to obtain rate constants and their temperature dependence for some consecutive reactions of higher alkynes that are formed in the reaction system O + C_2H_2 under acetylene rich conditions. A detailed study of this reaction at room temperature has been reported. The extension of this work to a temperature of 1300 K will be published in another paper [35].

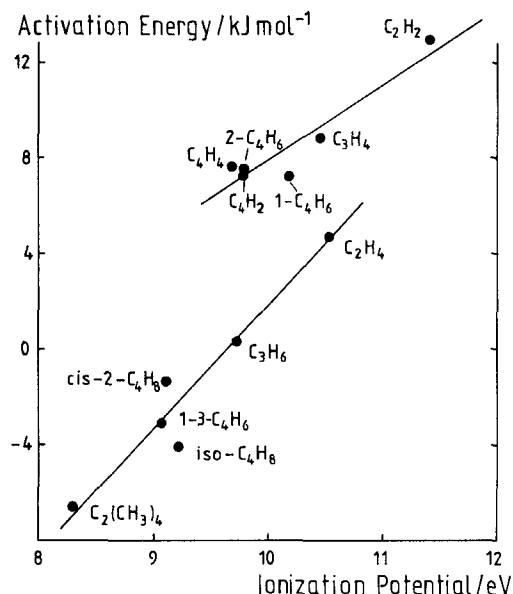


Fig. 7

Correlation between the activation energies of the reaction O + hydrocarbon and the ionization potential for some alkynes and alkenes [33]

This work received financial support from the Deutsche Forschungsgemeinschaft and the Fonds der Chemischen Industrie. This is gratefully acknowledged.

References

- [1] K. H. Homann and H. Schweinfurth, *Ber. Bunsenges. Phys. Chem.* **85**, 569 (1981).
- [2] K. H. Homann and H. Gg. Wagner, *Ber. Bunsenges. Phys. Chem.* **69**, 20 (1965).
- [3] K. H. Homann, G. Krome, and H. Gg. Wagner, *Ber. Bunsenges. Phys. Chem.* **72**, 998 (1968).
- [4] W. Schwanebeck and J. Warnatz, *Ber. Bunsenges. Phys. Chem.* **79**, 530 (1975).
- [5] K. H. Homann, W. C. Solomon, J. Warnatz, H. Gg. Wagner, and C. Zetsch, *Ber. Bunsenges. Phys. Chem.* **74**, 585 (1970).
- [6] W. Reppe, *Liebigs Ann. Chem.* **596**, 78 (1955).
- [7] J. C. Greaves and J. W. Linnett, *Trans. Faraday Soc.* **55**, 1355 (1959).
- [8] J. E. Morgan and H. I. Schiff, *J. Chem. Phys.* **38**, 1495 (1963).
- [9] D. S. Hacker, S. A. Marshall, and M. Steinberg, *J. Chem. Phys.* **35**, 1788 (1961).
- [10] A. A. Westenberg and N. de Haas, *J. Phys. Chem.* **73**, 1181 (1969).
- [11] K. H. Homann, J. Warnatz, and Ch. Wellmann, 16th Symp. (Internat.) on Combustion, p. 853, The Combustion Institute, Pittsburgh 1977.
- [12] B. Blumenberg, K. Hoyermann, and R. Sievert, 16th Symp. (Internat.) on Combustion, p. 841, The Combustion Institute, Pittsburgh 1977.
- [13] J. M. Brown and B. A. Thrush, *Trans. Faraday Soc.* **63**, 630 (1967).

- [14] C. A. Arrington, W. Brennen, G. P. Glass, J. V. Michael, and H. Niki, *J. Chem. Phys.* **43**, 525 (1965).
- [15] J. D. Sullivan and P. Warneck, *J. Phys. Chem.* **69**, 1749 (1965).
- [16] J. N. Bradley and R. S. Tse, *Trans. Faraday Soc.* **65**, 2685 (1969).
- [17] F. Stuhl and H. Niki, *J. Chem. Phys.* **55**, 3954 (1971).
- [18] I. T. N. Jones and K. D. Bayes, 14th Symp. (Internat.) on Combustion, p. 277, The Combustion Institute, Pittsburgh 1976.
- [19] C. V. Vinckier and W. Debruyne, 17th Symp. (Internat.) on Combustion, p. 623, The Combustion Institute, Pittsburgh 1978.
- [20] D. Saunders and J. Heicklen, *J. Phys. Chem.* **70**, 1950 (1966).
- [21] K. Hoyermann, H. Gg. Wagner, and J. Wolfrum, *Z. Phys. Chem. NF* **63**, 193 (1969).
- [22] G. S. James and G. P. Glass, *J. Chem. Phys.* **50**, 2268 (1969).
- [23] C. P. Fenimore and G. W. Jones, *J. Chem. Phys.* **39**, 1514 (1963).
- [24] W. G. Browne, R. P. Porter, J. D. Verlin, and A. H. Clark, 12th Symp. (Internat.) on Combustion, p. 1035, The Combustion Institute, Pittsburgh 1969.
- [25] J. Vandooren and P. J. Van Tiggelen, 16th Symp. (Internat.) on Combustion, p. 1133, The Combustion Institute, Pittsburgh 1977.
- [26] R. Löhr and P. Roth, *Ber. Bunsenges. Phys. Chem.* **85**, 153 (1981).
- [27] M. A. H. El-Dessouky, Dissertation, Univ. Göttingen 1970.
- [28] P. Herbrechtsmeier and H. Gg. Wagner, *Z. Phys. Chem. NF* **93**, 143 (1974).
- [29] C. A. Arrington, Jr. and D. J. Cox, *J. Phys. Chem.* **79**, 2584 (1975).
- [30] H. Niki and B. Weinstock, *J. Chem. Phys.* **45**, 3468 (1966); **47**, 3102 (1967).
- [31] K. H. Homann, W. Schwanebeck, and J. Warnatz, *Ber. Bunsenges. Phys. Chem.* **79**, 536 (1975).
- [32] P. Herbrechtsmeier and H. Gg. Wagner, *Ber. Bunsenges. Phys. Chem.* **79**, 461 (1975).
- [33] R. E. Huie and J. T. Herron, *Prog. React. Kinet.* **8**, 1 (1975).
- [34] D. D. Davis, R. E. Huie, and J. T. Herron, *J. Chem. Phys.* **59**, 628 (1973).
- [35] K. H. Homann and Ch. Wellmann, *Ber. Bunsenges. Phys. Chem.*, to be published 1983.

(Eingegangen am 3. März 1983)

E 5394

Measurements of Solubilities of Solid CO₂ in C₂H₄, C₃H₆, i-C₄H₈, n-C₅H₁₂ and of n-C₅H₁₂ in C₃H₆

Matthias Teller and Helmut Knapp

Institut für Thermodynamik und Anlagentechnik, Technische Universität Berlin

Lösungen / Phasengleichgewichte / Phasenumwandlungen / Stoffeigenschaften / Thermodynamik

Liquidus curves for five binary mixtures were determined in a low temperature equilibrium apparatus. It can be assumed that the solid phase consists of the pure solute. The experimental results were correlated and binary coefficients for a simple g^E model were calculated as a function of temperature.

Introduction

Knowledge about solid liquid equilibria (SLE) at low temperatures is required less as a basis for the design of crystallisation processes where pure solid substances are separated and produced but rather as a basis for the trouble free design of low temperature gas separation- and liquefaction-plants where the formation of solids causes plugging of flow passages. Gaseous mixtures found in nature such as air or natural gas or produced in chemical reactions such as refinery gas, coal gas or crack gas often contain components (e.g. H₂O, CO₂, H₂S, C₆H₆ etc.) with freezing points high in comparison to the liquefaction or freezing points of the other components (e.g. N₂, O₂, H₂, CO, CH₄ etc.). Such a component with a high freezing point can, when cooled down with the mixture, either solidify or dissolve in the otherwise fluids mixture.

When a low temperature plant is designed it is important to know whether components "freeze out" at any point. A solid-liquid equilibrium cell is operated at our institute in order to extend, supplement or check SLE-information.

Experimental Apparatus

A cell previously used for the investigation of SLE by Voss and Knapp [5] was redesigned (see Fig. 1). The double-wall metallic dewar 1 is evacuated through connection 2 to approx. 10^{-2} Pa. The cryostat is filled with 70 liters of a low boiling fluid e.g. N₂ for $70 \leq T \leq 95$ K, R13 for $95 \leq T \leq 120$ K, R12 for $115 \leq T \leq 290$ K. The level of the

bath liquid is indicated by a vertical rod 3 mounted on a float 4. The liquid is circulated by a propeller 5 driven by an electric motor via a magnetic clutch 6. The bath liquid is first cooled by liquid nitrogen introduced through vacuum insulated piping 7, evaporated in cooling coils 8 and warmed up in coils 9. The final adjustment of the bath temperature is accomplished by a temperature controlled electric heater 10.

The equilibrium cell 11 has a volume of 120 cm³ and is designed for a pressure of 150 bar. High pressure glass windows 12 allow the illumination and inspection of the interior of the cell. The cell has connections for the withdrawal of liquid samples through a capillary 13 and of vapor samples 14 as well as for filling. Two Pt-100 Ω temperature sensors are immersed into the cell 15. The liquid in the cell can be agitated by a propeller 16 driven via a magnetic clutch 17.

Instrumentation and Method of Measurement

The temperature is determined with calibrated platinum resistance thermometers by the current voltage method in combination with a digital multimeter with an accuracy of ± 0.05 K.

The pressure is measured with precision pressure gauges (Bourdon type, quality class 0.1). Four instruments with pressure ranges of 2, 6, 40 and 100 bar are used limiting the maximum error to 0.4 percent.

There are two experimental methods to determine a point on the liquidus curve (see Fig. 2):

- 1) A liquid solution of known composition is prepared. The liquidus line is passed by cooling or heating. The saturation temperature is determined by visual observation or by detection of thermal or optical effects.
- 2) A liquid solution is cooled down below the liquidus curve and samples of the saturated liquid are withdrawn and analysed e.g. by gaschromatography.